ACS SENSORS

Article

Cite This: ACS Sens. XXXX, XXX, XXX−XXX

pubs.acs.org/acssensors

Detection and Sourcing of Gluten in Grain with Multiple Floating-Gate Transistor Biosensors

Scott P. White, C. Daniel Frisbie, and Kevin D. Dorfman*

Department of Chemical Engineering and Materials Science, University of Minnesota − Twin Cities, 421 Washington Avenue SE, Minneapolis, Minnesota 55455, United States

Supporting Information

ABSTRACT: We report a chemically tunable electronic sensor for quantitation of gluten based on a floating-gate transistor (FGT) architecture. The FGTs are fabricated in parallel and each one is functionalized with a different chemical moiety designed to preferentially bind a specific grain source of gluten. The resulting set of FGT sensors can detect both wheat and barley gluten below the gluten-free limit of 20 ppm (w/w) while providing a source-dependent signature for improved accuracy. This label-free transduction method does not require any secondary binding events, resulting in a ca. 45 min reduction in analysis time relative to state-of-the-art ELISA kits with a simple and easily implemented workflow.

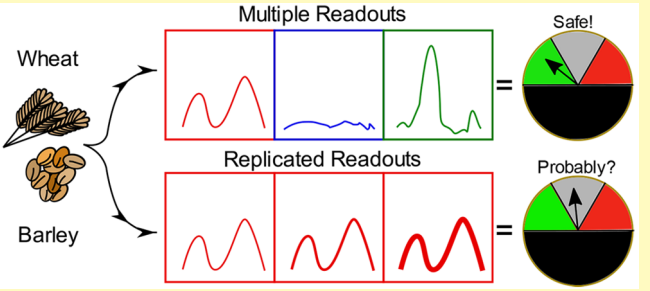

KEYWORDS: *printed electronics, microfluidics, gluten, biosensor, label-free*

Gluten is an umbrella term for a variety of storage proteins found in plants such as wheat, barley, and oats.[1,2] Gluten elicits an allergenic response in people who suffer from celiac disease, comprising ∼1% of the population.[3,4] Gluten exposure is a serious health issue for this population, whose collective hospital visits amount to thousands of dollars per patient (billions of dollars in total) due to dietary complications.[5,6] An additional ∼10% of the population is suspected to have at least a mild gluten sensitivity.[7]

Enzyme-linked immunosorbent assays (ELISA) are the dominant method for gluten detection,[8] but they suffer from poor quantitation,[9] inconsistencies in varied media,[10,11] and variability across manufacturers.[12] The analytical challenge arises from the variable chemistry of the gluten proteins found in the endosperm of plants such as wheat, barley, and some oats.[1,2] They all share chemical commonalities that trigger an allergenic response in celiac disease, but their structural chemistry varies as a function of plant source,[2,13] cultivar,[14] and processing conditions.[15] As a result, different antibodies, such as the Skerrit antibody,[16] the G12 antibody,[17] and the R5 antibody,[17] have been developed for gluten ELISA. Inevitably, different gluten sources have different dissociation constants for a given antibody,[18] making it challenging to establish a gluten-free limit of <20 ppm in all food sources using a single ELISA test. For example, the Skerrit antibody was developed from an immune reaction to ω-gliadin. While an excellent antibody for detecting ω-gliadin, the Skerrit antibody also binds other gluten sources.[16] When the Skerrit antibody is used as a generic binding agent for gluten, sources that are not dominantly ω-gliadin but otherwise above the gluten-free limit result in false negatives.[19]

The extraction of solid gluten proteins into a liquid matrix poses another considerable challenge.[18] Gluten is generally divided into two fractions: the ethanol soluble prolamin fraction and the insoluble glutenin fraction.[2,14,18] The ratio of these fractions in plants is assumed to be 1:1 but has been reported up to 1.5:1 or 1.7:1 in various conditions.[18] The convolution of the variability of the gluten chemistry and the variability of extracted proteins leads to significant variability when the same sample is tested using different gluten immunoassay kits, up to 50% or even 100%.[12]

The limitations in ELISA have motivated the development of new methods for gluten detection. One approach uses DNA-based sensors for cases where antibody-based methods fail due to changes during food processing, for example, during beer production.[20,21] A second approach replaces the antibody with a DNA aptamer having enhanced stability.[22,23] Impedimetric[24] and electrochemical[25] sensors using DNA aptamers for gluten have achieved improved limits of detection for common gluten samples when compared to conventional ELISA.[26,27] However, the sensitivity of a binding-based assay is always limited by the affinity of the binding agent for the target. If one wants to comprehensively assess the gluten content in food, more sophisticated proteomic methods that do not rely on affinity, such as mass spectrometry, are required[14,28,29] to overcome the limited reactivity of a single binding agent with classes of gluten samples that are not optimal for that binder.[26,30] In addition to detecting the presence of gluten, mass spectrometry can also

Received: November 2, 2017
Accepted: January 8, 2018

DOI: 10.1021/acssensors.7b00810
ACS Sens. XXXX, XXX, XXX−XXX

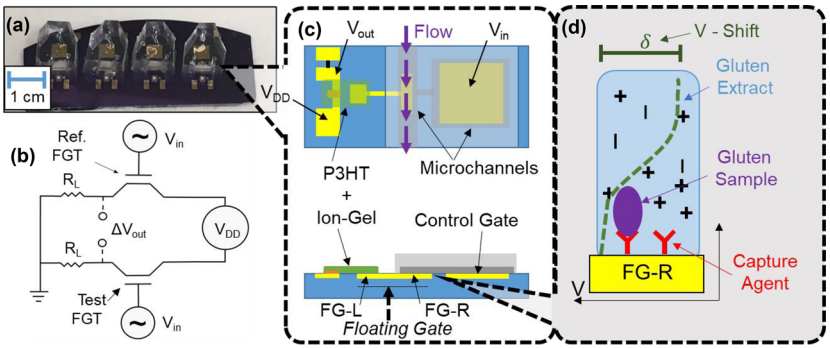

Figure 1. Device Architecture. (a) Photograph of a set of FGTs. (b) Equivalent circuit for a pair of FGTs that are placed in parallel with a load resistance (R_L) and a driving voltage (V_{DD}) set across them. The Reference FGT is functionalized with only PEG-ylated thiol while the Test FGT has PEG and chemical binders for gluten. The input voltage (V_{in}) modulates the conductivity of the FGTs and the response is read as a ΔV_{out} between the two sensors. (c) Schematic of a single FGT with materials and electrodes labeled along with the flow path of the sample. This is a simplified version of (b) representing only one side of the differential amplifier. (d) Schematic illustration of the active sensor surface with a capture agent (antibody or aptamer) on FG-R. The binding of gluten to the surface causes a change in the potential (green curve) that leads to a voltage shift. The *y*-axis qualitatively depicts the position away from the sensor interface.

provide information about the gluten source (e.g., wheat gluten or barley gluten). Unfortunately, current proteomic methods require a substantial increase in time, cost, and operator expertise relative to immunological methods, limiting their impact in practical applications.[20]

Motivated by the limitations of existing methods, we have developed an immunological assay based on floating gate transistors (FGTs) that bridges the gap between ELISA and mass spectrometry.[12,14,20] Compared to commercial ELISA kits, our method better quantifies gluten in less time, while also being far easier to use than mass spectrometers due to the minimal number of processing steps and automated sample handling. We have previously shown how this rapid FGT biosensing technology, which combines printed electronics and microfluidics, leads to a label-free, potentiometric transducer for sensing biomacromolecules such as DNA[31] and proteins.[32,33] In contrast to conventional ELISA methods, the FGT signal depends on intrinsic changes at the sensor surface. As a result, secondary binding events[12,34] are not necessary. Removing the secondary binding step reduces the time to transduction by at least 30 min (of a total 45 min reduction relative to ELISA), an improvement similar to advanced microfluidic-ELISAs,[35] and also circumvents problems when the secondary epitope is altered during processing, for example, when cooking food. Eliminating the need for a secondary binding event also permits detection directly from gluten extraction cocktails, which contain high concentrations of reducing agents that can sometimes interfere with complex protein−protein ligand binding, thereby minimizing the reaction time.[18] The device design utilizes a small active area (<1 mm^2) and corresponding small sample volumes (<100 μL). This presents a volume reduction of 3−5× relative to ELISA kits. The set of FGT sensors developed here represent a developmental improvement of immunoassays analogous to those by Luminex Multiplex Assays[36,37] but with streamlined manufacturing and operating protocols. By systematically altering the binding chemistry of the sensor and comparing the response as a function of gluten source, we demonstrate that our approach not only can determine the presence of gluten, but also has the sensitivity to provide a chemical fingerprint for the gluten source.

EXPERIMENTAL METHODS

Materials. Poly(3-hexylthiophene) (P3HT) was purchased from Rieke Metals, Inc. and stored in an inert environment. 1-Ethylmethyl imidazolium bis(trifluoromethyl)sulfonylimide (EMIM/TFSI) was purchased from EMD Millipore, Inc. and stored in an inert environment. Polystyrene-*b*-methyl methacrylate-*b*-styrene (SMS) was synthesized by a previously reported procedure by Zhang et al.[38] The ion-gel was a mixture of SMS and EMIM/TFSI at 1:9 by weight.

Gliadin (PWG) was purchased from Prolamin Working Group as a mixture of various plant sources.[39] Wheat gluten and barley gluten were obtained from a local co-op as ground baking ingredients. The gli4 aptamer developed by Amaya-Gonzalez et al.[22] was purchased from Integrated DNA Technologies with the sequence: HS-C_6H_{12}-5′-CCA-GTC-TCC-CGT-TTA-CCG-CGC-CTA-CAC-ATG-TCT-GAA-TGC-C-3′. Wheat antibody G12 was purchased from Biomedal. A custom barley antibody (BAb) was obtained from Pacific Immunology Inc. by sending them the barley extract (from the local co-op baking ingredient) and receiving the purified immune response of rabbits. The gluten extraction matrix (often referred to as a "cocktail") was an established recipe[18] comprising 250 mM of β-mercaptohexanol (Sigma-Aldrich) and 2 M guanidine HCl (Sigma-Aldrich). 11-Mercaptoundecanoic acid and poly(ethylene glycol) methyl ethyl thiol (PEG-ylated thiol, M_n = 800) were purchased from Sigma-Aldrich and used as received.

Device Fabrication. Devices were fabricated using the printing process reported previously[40] by first photolithographically patterning Cr/Au electrodes (5 nm/30 nm) and then printing the organic materials with an Aerosol-Jet 200 Printer (Optomec, Inc.) using a 150 μm nozzle. For printing, P3HT was dissolved first in chloroform at 1 mg/mL and then terpineol was added as a cosolvent at 0.1 mL per mL of chloroform solution. The solution was printed using a carrier gas flow rate of 10 ccm and a sheath gas flow rate of 20 ccm. The ion-gel was mixed with ethyl acetate at a ratio of 1:9 by weight, stirred overnight, and then printed using a carrier gas flow rate of 20 ccm and a sheath gas flow of 25 ccm. Poly(styrene) was dissolved in chloroform and terpineol (10:1 by volume) at a concentration of 5 mg/mL at a carrier gas flow rate of 20 ccm and a sheath gas flow rate of 30 ccm. More details on the printing process have been reported previously.[40]

Microfluidics. Microfluidic flow channels were imprinted into poly(dimethylsiloxane) (PDMS) molds from an SU8 master.[41] The base and curing agent were poured onto the SU8 master at a ratio of 10:1 then heated at 75 °C for 2 h. The imprints were 150 μm high in a pattern that outlined the right arm of the floating-gate electrode (FG-R, Figure 1C) and the control gate electrode. The imprints over the floating-gate electrode were extended to one inlet port and one outlet port such that a solution injected through the inlet flows over FG-R.

DOI: 10.1021/acssensors.7b00810
ACS Sens. XXXX, XXX, XXX−XXX

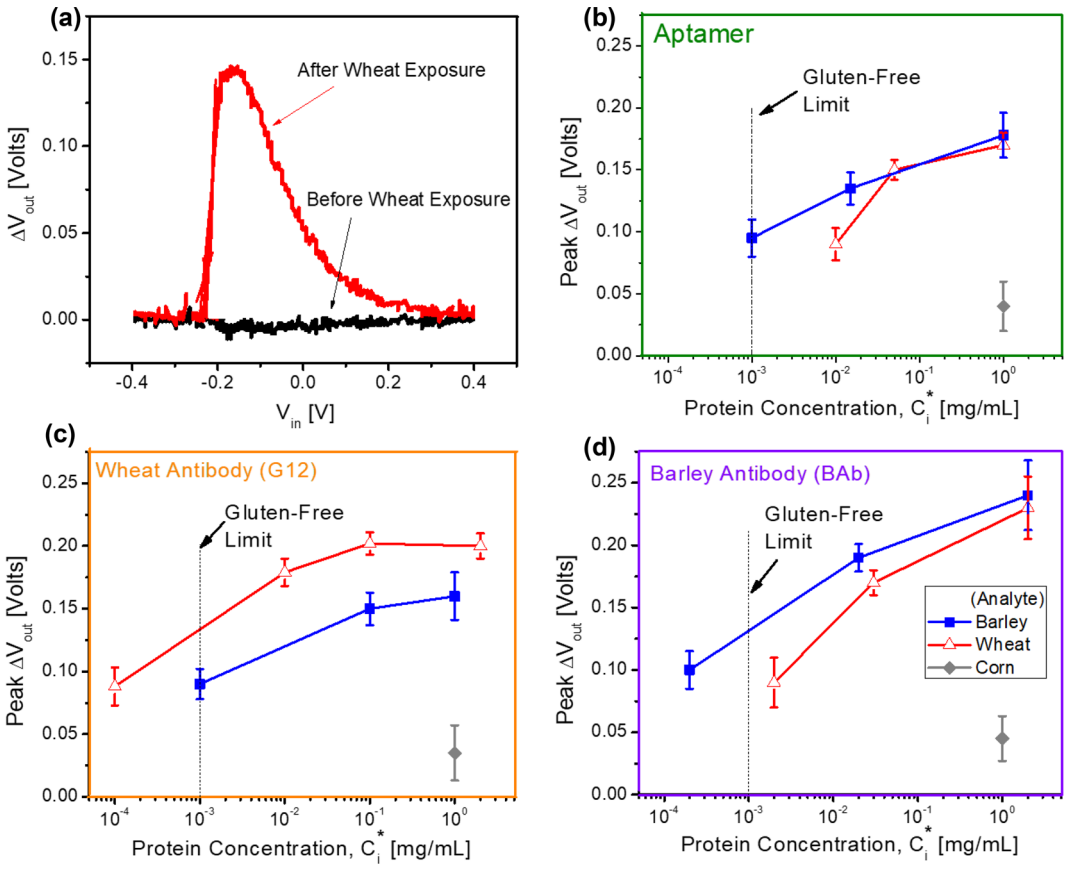

Figure 2. FGT Response. (a) Example of the device response of an FGT functionalized with aptamers and exposed to wheat at 0.1 mg/mL. The curves are averaged over 5−10 min of testing. Dose−response curves for (b) an aptamer-functionalized FGT, (c) a G12-functionalized FGT, and (d) a BAb-functionalized FGT when exposed to the wheat (red open triangles), barley (blue closed squares), and gluten-free corn (gray diamonds). Error bars are the standard deviation for 3 devices. The gluten concentrations on the *x*-axis of (b)-(d) are given by eq 1 at various dilutions as determined by a GlutenTox ELISA kit.

Another inlet was imprinted above the control gate so that solution flows over the control gate to the outlet.[33]

Interface Functionalization. Once fabricated, FG-R was cleaned by flowing sodium borohydride at 1.0 μL/min and 0.5 M for 1 h, then rinsed with distilled water.

For aptamer functionalization, aptamers were dissolved in Tris buffer with 0.1 M NaCl at 1 μM and flowed over FG-R overnight (>16 h), leading to a coverage of ∼2 pmol/cm^2.[42] PEG-ylated thiol was then dissolved in distilled water at 1 mM and flowed over FG-R and the Control Gate at 1.0 μL/min for 2 h. Finally, the interface was rinsed with buffer.

For antibody conjugation, FG-R was functionalized first with 11-mercaptoundecanoic acid (−COOH) and PEG-ylated thiol at a concentration of 1 mM in ethanol/water (50/50 v/v) and an acid:PEG ratio of 1:9. The surface was rinsed and then reacted with 1-ethyl-3-(3-(dimethylamino)propyl)carbodiimide hydrochloride (EDC) at 5 mM and *N*-hydroxysuccinimide (NHS) at 2 mM in MES buffer for 15 min. Following the reaction, the surface was rinsed with phosphate buffered saline solution. The activated surface was then exposed to an antibody solution at a concentration of 0.1 mg/mL for 2 h to form an amide bond with the −COOH groups on the electrode surface.[43] The concentration of the protein solutions was confirmed using a Thermo-Fisher Nanodrop to measure the absorbance of protein solutions at 280 nm.

These strategies were used to fabricate the Test Sensor. The Reference Sensor was fabricated in the same manner but without aptamers (or antibodies), so that only the PEG-ylated thiol blocking layer was on the floating gate.

Testing Protocol. The gluten samples were extracted with the extraction cocktail following established protocols.[18] For the PWG gliadin sample, the powder was simply massed and then diluted to a desired concentration followed by vortex mixing. For the wheat and barley samples, 100 mg were massed and then diluted in 1 mL of extraction cocktail, vortexed, allowed to dissolve at room temperature for 30 min, and centrifuged for 10 min. The resulting solution was diluted to the desired protein concentration based on the gluten concentration determined by ELISA.

To measure a baseline, the microfluidic channels on a test and reference FGT were first filled with extraction cocktail without any gluten sample. An input voltage, $V_{in} = V_0 + V_1 \sin(\omega t)$, was applied to the control gate of each device (Figure 1C). At the same time, the output voltage between the transistor and the resistor (R_L = 1 MΩ) in Figure 1C was measured. V_1 was fixed at 0.4 V, while V_0 was tuned so that the resistance of the transistor was equal to R_L when $V_{in} = V_0$. Typically, this requires that V_0 be between −0.3 V and +0.3 V. The resulting $\Delta V_{out} = V_{out,\ Test\ FGT} - V_{out,\ ref.\ FGT}$ is then approximately zero for all V_{in}. The frequency is ω = 13 Hz. The measurement was repeated 5−10 times at a rate of once per min. This procedure is very similar to that reported elsewhere.[33]

The equivalent circuit for our device is outlined in Figure 1B. The resulting ΔV_{out} waveforms are averaged and recorded as the "blank" in Figure 2A. This step occurs during the centrifugation or dissolution of the gluten sample.

In the second step of the measurement, FG-R was exposed to the gluten sample through microfluidic sample delivery for 30 min at a rate of 1 μL/min, and then rinsed with blank extraction cocktail. The flow was stopped and then the same input waveform used in the first step was applied for 5−10 min at a rate of once per min. The resulting ΔV_{out} waveforms were averaged and the peak ΔV_{out} was recorded as the signal corresponding to the input concentration of gluten.

DOI: 10.1021/acssensors.7b00810
ACS Sens. XXXX, XXX, XXX−XXX

ELISA. GlutenTox Sandwich ELISA kits were purchased from Biomedal and used according to the manufacturer protocol.[34]

RESULTS

The FGT biosensor is depicted in Figure 1. The sensors are fabricated in parallel with each "pixel" defined by the chemistry of the sensor surface (Figure 1A). The core of the sensor is a floating gate electrode with two arms. The left arm (FG-L) is connected to a printed semiconductor (poly(3-hexylthiophene) or P3HT) via an ion-gel electrolyte that permits very low voltage operation (<1 V) (Figure 1A-C).[31,33,40] The right arm (FG-R) is connected to the microfluidic network via an aqueous electrolyte that, in this work, is an extraction cocktail that solubilizes gluten proteins in food samples (250 mM of β-mercaptohexanol and 2 M of guanidine HCl in water).[18] The gluten extract is contained by PDMS microchannels that guide the flow of the sample over FG-R only (Figure 1C). The flow decreases the binding time relative to ELISA by at least 15 min.[35]

The sensor surface on FG-R is functionalized to specifically capture gluten from the extract while minimizing nonspecific adsorption. The capture agents were (i) an aptamer (gli4) designed to bind the active 33-mer epitope of gluten developed by Amaya-Gonzalez et al.;[23,26] (ii) the commercially available G12 antibody generated to bind wheat gluten;[17] or (iii) a custom barley antibody developed by Pacific Immunology Inc. (BAb).

Upon binding, the gluten proteins are concentrated at the sensor surface, raising the interfacial charge;[32] the high proline content of soluble gluten renders it negatively charged at neutral pH.[2] This alteration in interfacial charge distribution changes the surface potential relative to the bulk of the aqueous electrolyte, illustrated schematically by the voltage shift δ in Figure 1D.[41] The potentiometric perturbation alters the output of the device at a given V_{in}. The experiment is conducted on a Test Sensor and a Reference Sensor in parallel, leading to the equivalent circuit in Figure 1B. The output of the device is obtained as the difference between the responses of the two devices, which we denote as ΔV_{out}.

For our experiments, we would like to determine the relationship between ΔV_{out} and the gluten concentration. This requires knowledge of the mass fraction of gluten in the grain sample and the solubility factor

$$C_i^* = \frac{m_0 X_0 f_0}{(1 + D)V_0} \quad (1)$$

where m_0 is the mass of grain, V_0 is the volume of extraction cocktail, f_0 is the fraction of gluten that is soluble in the extraction cocktail (assumed to be 0.5 here[2]), X_0 is the weight fraction of gluten in the stock (w/w) determined from standard ELISA kits, D is the dilution, and C_i^* is referred to as the "true concentration" of gluten exposed to an FGT with functionalization i (i = Apt, G12, or BAb). We used two sources of grain gluten: wheat and barley. The gluten mass fractions of these sources were measured with a GlutenTox ELISA kit to be X_0^W = 1.3% (w/w) in wheat and X_0^B = 0.5% (w/w) in barley.[34] Due to this disparity in gluten concentrations of the food material, the extracted supernatants were diluted differently (see Methods) in order to set the gluten concentration C_i^* exposed to the sensor to be within the desired range.

Note that, with this protocol, we are operating under the assumption that the ELISA kit provides an accurate measure of X_0. Ultimately this is not a limitation in our method, as it simply provides a convenient standard for plotting the gluten concentrations for the data that follow. We will discuss shortly how to operate the sensor without the need to calibrate it with an ELISA measurement.

Figure 2A shows the device output for a specific example where FG-R was functionalized with the gli4 aptamer. In these experiments, the microchannels were filled first with a blank extraction cocktail. A supply voltage of +0.5 V was input at V_{DD}. The input voltage at the control gate was swept from +0.4 V to −0.4 V around a DC bias. The value of the DC bias was tuned for each device to maximize the gain of the differential amplifier scheme and is 0.0 V for the example in Figure 2A. The output voltage is measured at V_{out} (Figure 1C), using a 1 MΩ resistor (R_L) in series. The black data in Figure 2A show the averaged result of this measurement of a blank sample. The individual curves vary about zero with fluctuations of ∼25 mV (see Supporting Information). Following this baseline measurement, FG-R was exposed to a gluten sample for 30 min. In this experiment, the sample was gluten extracted from wheat and diluted to a concentration of C_i^* = 0.1 mg/mL. The red data in Figure 2A show the output of the device when exposed to the gluten sample. The displayed curve is constructed by subtracting the output of the reference device from the test device each min for 5−10 min and then averaging the resulting curves. The maximum value of the red waveform is the value of ΔV_{out}; we thus conclude that ΔV_{out} = 0.15 V for wheat gluten at C_i^*= 0.1 mg/mL using an aptamer-functionalized FGT. The measured peak value of ΔV_{out} is used for analysis because (i) it is stable, being the result of an average of the output waveforms over each voltage sweep; (ii) it better correlates with gluten concentration relative to alternatives (e.g., area of the ΔV_{out} waveform, width of waveform); and (iii) it is very simple to determine.

We repeated these measurements for different gluten sources over several orders of magnitude of total protein concentration using two antibodies and a DNA aptamer. For each gluten source and binding agent, the FGT response was measured (i) at the limit of detection (0.1−1.0 μg/mL); (ii) above the gluten-free limit (10−100 μg/mL); and (iii) at a very high concentration outside the quantitation regime (≥1 mg/mL). The limit of detection is defined as three times the voltage fluctuations observed during the blank run (see Supporting Information). The fluctuations are caused by variations in the device threshold voltage, drift at the control gate, and streaming currents created by spurious flow of the electrolyte. As a control experiment, we also used corn (non-celiac-active) as a gluten-free food sample. Control experiments measured signals that would correspond to gluten samples at 3−4 orders of magnitude lower concentration.

The aggregated data are shown in Figure 2: aptamers in Figure 2B (green highlight), wheat antibody (G12) in Figure 2C (orange highlight), and barley antibody (BAb) in Figure 2D (magenta highlight). Each sensor was exposed to two different sources of grain: ground wheat from a local co-op (red open triangles), and ground barley flakes from a local co-op (blue squares) yielding the six curves shown in Figures 2B-D. The concentration displayed on the x-axis of Figure 2B-D, C_i^*, corresponds to the value we expect to have in the solution based on the gluten content measured by ELISA following eq 1. The gluten in the samples was detectable below the gluten free limit on one of the three types of FGT sensors. With the exception of the detection of wheat using the G12 antibody

DOI: 10.1021/acssensors.7b00810
ACS Sens. XXXX, XXX, XXX−XXX

(Figure 2C), we obtained points that appear to be in the quantitative regime of each sensor. Rigorously pinpointing these boundaries would require ~5−10× more data, and the concomitant technological advancements that will enable the requisite higher throughput for both device manufacture and measurement will be a focus of future work.

DISCUSSION

Figure 2 makes it clear that the value of the measured signal ΔV_{out} for a given capture agent depends on the gluten source. For example, in Figure 2C (orange border), the wheat antibody elicited the strongest response from wheat and a considerably lower response to barley. The opposite trend is observed in Figure 2D (magenta border) with BAb eliciting a stronger response to barley relative to wheat. These results are expected, as these antibodies were developed to best bind a particular gluten source. The shape of the curves is governed by two nonlinear aspects of the FGT transduction: (i) the nonlinear relationship between gluten dissolved in the solution and surface bound gluten (i.e., the adsorption isotherm) and (ii) the nonlinear relation between surface bound gluten and the potential shift. This behavior is consistent with previous reports[33] and currently under further investigation.

The dependence of the signal on the gluten source can be exploited to source the gluten in a sample. In order to execute this task, the measured signals need to be compared to a reference material within the quantitation regime of the respective dose−response curves. There is no consensus reference material for gluten,[39] so we used the PWG gliadin in order to discriminate the relative signals from wheat and barley samples.

Figure 3 is the calibration curve with PWG exposed to each FGT type at various dilutions. The x-axis is presented as a protein concentration that refers to the concentration of the PWG standard obtained from eq 1 with the assumptions that the PWG solid is 100% gluten and completely soluble (X_0^{PWG} = 1.0, f_0^{PWG} = 1.0). The curves in Figure 3 correspond to the different FGT functionalizations (green filled circles for aptamers, orange half-filled circles for G12, and magenta open circles for BAb). Note that the curves in Figure 3 overlap much more than those in Figure 2, reflecting the utility of using PWG across many gluten binders and the reason why PWG has been adopted in many studies as a reference gluten material. Each type of FGT sensor is able to detect gluten at or below the gluten-free limit of 10^{-3} mg/mL (20 ppm).

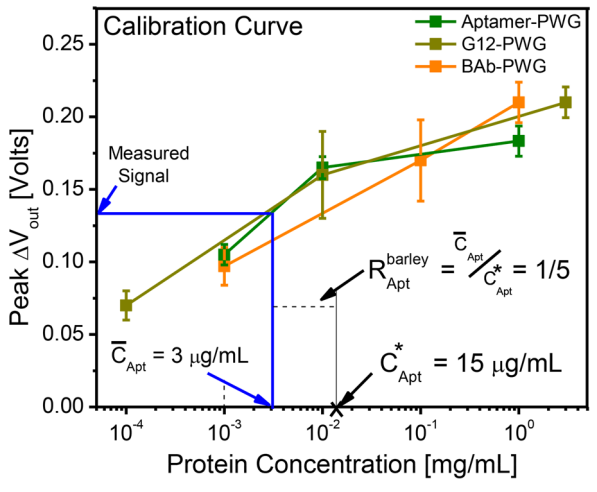

Figure 3. Calibration Curve. The peak ΔV_{out} is plotted with respect to the PWG protein concentration for the three different binders: aptamers in green, G12 antibody in olive, and BAb in orange. An example is shown in blue where the measured signal for a barley sample is connected to a measured concentration, $\bar{C}_i$, that is 5× lower than the concentration, C_i^*, determined by reference to ELISA with eq 1.

We can use the data in Figure 2 and Figure 3 to construct a fingerprint for the gluten source based on the measurement disparity between the FGT with functionalization i and the concentration C_i^* obtained from ELISA and eq 1. To do so, we assume that we know the relevant boundaries of the quantitation regimes for each binder-analyte pair. In this regime the measurement disparity depends only on the gluten source not the (unknown) concentration. The signal ΔV_{out} from FGT functionalization i when exposed to a gluten concentration C_i^*, can be compared to the concentration of PWG, $\bar{C}_i$, that elicits the same signal ΔV_{out} from FGT functionalization i. A concrete example is indicated by the blue line in Figure 3 where the ΔV_{out} that corresponds to C_{Apt}^* = 15 μg/mL when the aptamer-functionalized FGT is exposed to barley gluten (Figure 2B) produces $\bar{C}_{Apt}$ = 3.0 μg/mL for a similar aptamer-functionalized FGT exposed to PWG. This disparity is represented by the ratio

$$R_i^s = \bar{C}_i / C_i^* \tag{2}$$

where R_i^s refers to the disparity from FGT functionalization i when it exposed to gluten from grain source s. The example in Figure 3 yields $R_{Apt}^{barley} = \bar{C}_{Apt}/C_{Apt}^* = 1/5$, assuming both $\bar{C}_{Apt}$ and C_{Apt}^* lie in the quantitation regime of their respective curves. A low value of R_i^s (<1) means the FGT functionalization i more strongly prefers the PWG standard relative to the target gluten s because a larger amount grain gluten (C_{Apt}^*) is required to elicit the same FGT signal as the PWG ($\bar{C}_{Apt}$) for FGT type i.

Figure 4 presents the resulting signal disparities from eq 2 as a function of FGT functionalization and gluten source, which we can interpret as chemical signatures for wheat and barley produced by the FGT sensor. The inset shows the concentration of gluten exposed to the sensors (C_i^*) for the

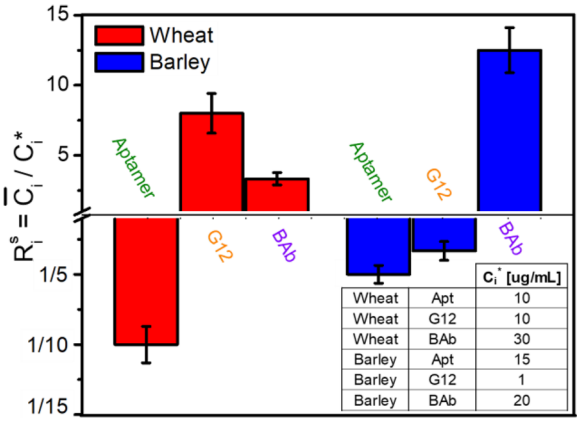

Figure 4. Gluten Signatures. The resulting ratios (R_i^s) of measured concentration ($\bar{C}_i$) relative to the reference concentration (C_i^*) are presented when the set of FGTs are exposed to wheat gluten (red bars) and barley gluten (blue bars). Up-oriented bars represent a stronger preference for wheat/barley relative to the PWG standard. The inset lists the reference concentrations (C_i^*) used from Figure 2.

DOI: 10.1021/acssensors.7b00810
ACS Sens. XXXX, XXX, XXX−XXX

disparity calculation and is assumed to reside in the quantitation regime of the sensors (C_i^* = 1−30 μg/mL). For clarity, ratios less than one are oriented downwards. With this convention, a large up-oriented bar means the FGT functionalization binds more strongly to the gluten source relative to the PWG reference. A down-oriented bar means the FGT functionalization binds more strongly to the PWG. The red bars represent the disparities from wheat gluten and highlight the preference of G12 and BAb to bind wheat gluten relative to the PWG reference while the opposite is true for aptamers. The blue bars represent the disparities for barley gluten and highlight the ability of BAb to strongly transduce barley gluten relative to the reference PWG while both aptamers and G12 prefer the PWG reference.

The phenomenon in Figure 4 arises naturally from the procedures used to synthesize the different binders.[16,17,22,23] The custom barley antibody (BAb) was extracted from an immunogenic response to the very same barley source used in this report. As such, it binds much more strongly to the barley gluten relative to the other analytes.[23] However, this strong specificity is expected to be very limited and should not be extrapolated to other sources of gluten, even other barley sources of gluten. The G12 functionalized FGT yields the strongest response to wheat gluten which also reflects the origin of the binder as a product of an immune response to wheat gluten.[17] Unlike the BAb, the wheat source for G12 was more generalizable resulting in a broader reactivity profile for G12 compared to BAb and relatively lower preference for G12 compared to the preference of BAb to barley. The aptamers exhibit a slightly lower sensitivity relative to antibodies. This is likely due to a combination of a weaker binding affinity with the processed gluten or different molecular transduction between aptamers and antibodies. In isolation, these binder features have their pros and cons but a set of sensors can leverage them to simultaneously assess the source and amount of gluten under investigation.[30,36]

For routine analysis, using a set of functionalized FGTs can improve further the accuracy of gluten quantitation by combining the disparities in Figure 4 with the raw device responses in Figure 2 and Figure 3. When exposed to an unknown amount of gluten from an unknown grain source, C, the set of FGT sensors will yield three values of $\overline{C}_i$ that can be extracted from the known calibration curves (Figure 3). The measured values of $\overline{C}_i$ can be then be equated to C with disparities, $\overline{R}_i = \overline{C}_i/C$,

$$\overline{C}_i = \overline{R}_i C \qquad \text{for } i = 1, 2, ..., n \tag{3}$$

Equation 3 is valid provided the measured values of $\overline{C}_i$ are in the quantitation regime. This is not a particularly strong restriction, since its satisfaction can be ensured through serial dilutions of a high concentration sample. With an unknown value of C, eq 3 is underspecified, having n independent equations for n + 1 unknowns, in effect leaving the unknown concentration undefined. In this work we used n = 3 but the procedure is generalizable to an arbitrary number of FGT functionalizations.

To estimate the unknown concentration C, as well as the source of gluten, we also require a library of k reference R_i^s values, such as what we obtained in Figure 4 using k = 2 gluten sources and three FGT functionalizations. To complete the set of equations, we vary C such that the resulting disparities satisfy

$$\min \sum_i (\overline{R}_i - R_i^S)^2 \tag{4}$$

for each source s in the library, yielding k estimates for C and residuals from eq 4 corresponding to each of those k estimates. The source s whose minimization yields the smallest residual is identified as the source of the gluten, and the corresponding value of C from that minimization is the gluten concentration.

The resulting value of C will be more accurate than any of the measured values, $\overline{C}_i$, because it properly accounts for the disparity in measurements due to source-dependent gluten chemistry. Additionally, the set of R_i^s in Figure 4 that minimizes the error provides strong evidence of the source of the gluten sample which can be useful for identifying the cause of an unexpected contamination. Naturally, this approach improves as the size k of the library increases. With a sufficient database of gluten signatures, the set of FGTs does not need to be calibrated with respect to an ELISA kit, as in Figure 2, to determine the gluten concentration.

In food safety applications, choosing an appropriate set of functionalized FGTs can minimize both false negatives and false positives. For example, if an unknown sample yielded $\overline{C}_i$ values both above or below the gluten-free limit then the set of $\overline{R}_i$ found from eq 3 would result in a more accurate measure of concentration C that pinpoints it in the proper regime. This practice also alleviates the challenge of identifying a proper gluten reference material provided the standard used in the FGT kit has previously been calibrated using a more accurate proteomic method.[39] While we used ELISA as the benchmark to produce the data in Figure 4, one could use a more sophisticated method such as mass spectrometry to produce more reliable data for the library of R_i^s values.

CONCLUSIONS

In this work, we have leveraged the parallelizability and versatility of FGTs to create a set of sensors for gluten detection and sourcing. In the present prototype method, the analysis takes ∼1.5 h to quantify a raw food sample—a reduction of ∼45 min compared to the commercial, optimized ELISA kits, such as the one that we used to provide the reference measurements of gluten in Figure 2. The current set of FGT sensors incorporates three binders and we showed that it can detect and source gluten from two different samples. Intuitively, the accuracy of gluten sourcing will increase by increasing the number of binders in the FGT set. In practice, the number of binders necessary to differentiate gluten sources is expected to be approximately equal to the number of potential sources of the unknown gluten. However, this can be increased or decreased depending on the end application and required confidence when sourcing.

At present, the materials cost for the set of FGTs is estimated to be about ∼3× lower than the cost of a single ELISA kit, and ∼10× lower than a set of ELISA kits that would be needed to assess the binding disparities in the same fashion. Further reductions in FGT cost could be realized at higher production scales. The specific design of the FGT set is a trade-off between the cost, the number of potential source contaminants, and the accuracy required to confidently differentiate between these sources.

More concrete delineation between gluten sources will be a subject of future work, including analyzing mixtures of different gluten sources and determining the ability for FGT sets of various sizes to differentiate between them. Further work will

DOI: 10.1021/acssensors.7b00810
ACS Sens. XXXX, XXX, XXX−XXX

also compartmentalize the electronics equipment and fluidic handling system in order to parallelize the measurement protocols to create a fully multiplexed FGT sensor for gluten. In such a device, the time and effort required to measure the response at one FGT pixel will be equivalent to the measurement of *n* FGTs. The dose−response curves in Figure 2 will be further resolved and the signal disparities for other gluten sources (e.g., oats) will be combined to the signatures in Figure 4. The expanded capabilities will advance the analytical capabilities of the food sector leading to safer products for the public.[30]

■ ASSOCIATED CONTENT

Supporting Information

The Supporting Information is available free of charge on the ACS Publications website at DOI: 10.1021/acssensors.7b00810.

Individual traces of an FGT as they are exposed to wheat gluten. The traces were used to construct the average traces in Figure 2A. (PDF)

■ AUTHOR INFORMATION

Corresponding Author

*E-mail: dorfman@umn.edu.

ORCID

Scott P. White: 0000-0001-9396-0067

Kevin D. Dorfman: 0000-0003-0065-5157

Notes

The authors declare the following competing financial interest(s): The authors are founders of Printed Bioelectronic Solutions, which intends to commercialize EGT sensor technologies.

■ ACKNOWLEDGMENTS

We acknowledge funding from the National Science Foundation (Predoctoral Fellowship for SPW), the University of Minnesota MN-Drive program, and the Office of Naval Research through the Multi-University Research Initiative (CDF). A portion of this work was performed at the University of Minnesota Nanofabrication Center which received partial support from the NSF through NNIN.

■ REFERENCES

(1) Shewry, P. R.; Halford, N. G.; Belton, P. S.; Tatham, A. S. The Structure and Properties of Gluten: An Elastic Protein from Wheat Grain. *Philos. Trans. R. Soc., B* **2002**, *357* (1418), 133−142.

(2) Wieser, H. Chemistry of Gluten Proteins. *Food Microbiol.* **2007**, *24* (2), 115−119.

(3) Leonard, M. M.; Sapone, A.; Catassi, C.; Fasano, A. Celiac Disease and Nonceliac Gluten Sensitivity. *JAMA* **2017**, *318* (7), 647−656.

(4) Ch'ng, C. L.; Jones, M. K.; Kingham, J. G. C. Celiac Disease and Autoimmune Thyroid Disease. *Clin. Med. Res.* **2007**, *5* (3), 184−192.

(5) Ross, M. P.; Ferguson, M.; Street, D.; Klontz, K.; Schroeder, T.; Luccioli, S. Analysis of Food-Allergic and Anaphylactic Events in the National Electronic Injury Surveillance System. *J. Allergy Clin. Immunol.* **2008**, *121* (1), 166−171.

(6) Long, K. H.; Rubio-Tapia, A.; Wagie, A. E.; Melton, L. J., III; Lahr, B. D.; Van Dyke, C. T.; Murray, J. A. The Economics of Celiac Disease: A Population-Based Study. *Aliment. Pharmacol. Ther.* **2010**, *32* (2), 261−269.

(7) Castillo, N. E.; Theethira, T. G.; Leffler, D. A. The Present and the Future in the Diagnosis and Management of Celiac Disease. *Gastroenterol. Rep.* **2015**, *3* (1), 3−11.

(8) Haraszi, R.; Chassaigne, H.; Maquet, A.; Ulberth, F. Analytical Methods for Detection of Gluten in Food–Method Developments in Support of Food Labeling Legislation. *J. AOAC Int.* **2011**, *94* (4), 1006−1025.

(9) Scherf, K. A.; Poms, R. E. Recent Developments in Analytical Methods for Tracing Gluten. *J. Cereal Sci.* **2016**, *67*, 112−122.

(10) Van Boekel, M. A. J. S. Kinetic Modeling of Food Quality: A Critical Review. *Compr. Rev. Food Sci. Food Saf.* **2008**, *7* (1), 144−158.

(11) Poms, R. E.; Klein, C. L.; Anklam, E. Methods for Allergen Analysis in Food: A Review. *Food Addit. Contam.* **2004**, *21* (1), 1−31.

(12) Bruins Slot, I. D.; Bremer, M. G. E. G.; van der Fels-Klerx, I.; Hamer, R. J. Evaluating the Performance of Gluten ELISA Test Kits: The Numbers Do Not Tell the Tale. *Cereal Chem.* **2015**, *92* (5), 513−521.

(13) Rallabhandi, P.; Sharma, G. M.; Pereira, M.; Williams, K. M. Immunological Characterization of the Gluten Fractions and Their Hydrolysates from Wheat, Rye and Barley. *J. Agric. Food Chem.* **2015**, *63* (6), 1825−1832.

(14) Alves, T. O.; D'Almeida, C. T. S.; Ferreira, M. S. L. Determination of Gluten Peptides Associated with Celiac Disease by Mass Spectrometry, Celiac Disease and Non-Celiac Gluten Sensitivity, Rodrigo, L., Ed.; InTech, 2017. DOI: 10.5772/67547.

(15) Rallabhandi, P. Gluten and Celiac Disease—An Immunological Perspective. *J. AOAC Int.* **2012**, *95* (2), 349−355.

(16) Skerritt, J. H.; Hill, A. S. Monoclonal antibody sandwich enzyme immunoassays for determination of gluten in foods. *J. Agric. Food Chem.* **1990**, *38* (8), 1771−1778.

(17) Hochegger, R.; Mayer, W.; Prochaska, M. Comparison of R5 and G12 Antibody-Based ELISA Used for the Determination of the Gluten Content in Official Food Samples. *Foods* **2015**, *4* (4), 654−664.

(18) García, E.; Llorente, M.; Hernando, A.; Kieffer, R.; Wieser, H.; Méndez, E. Development of a General Procedure for Complete Extraction of Gliadins for Heat Processed and Unheated Foods. *Eur. J. Gastroenterol. Hepatol.* **2005**, *17* (5), 529−539.

(19) Collin, P.; Mäki, M.; Kaukinen, K. Safe Gluten Threshold for Patients with Celiac Disease: Some Patients Are More Tolerant than Others. *Am. J. Clin. Nutr.* **2007**, *86* (1), 260.

(20) Tanner, G. J.; Colgrave, M. L.; Blundell, M. J.; Goswami, H. P.; Howitt, C. A. Measuring Hordein (Gluten) in Beer − A Comparison of ELISA and Mass Spectrometry. *PLoS One* **2013**, *8* (2), e56452.

(21) Martín-Fernández, B.; de-los-Santos-Álvarez, N.; Martín-Clemente, J. P.; Lobo-Castañón, M. J.; López-Ruiz, B. Challenging Genosensors in Food Samples: The Case of Gluten Determination in Highly Processed Samples. *Talanta* **2016**, *146*, 490−495.

(22) Amaya-González, S.; de-Los-Santos-Álvarez, N.; Miranda-Ordieres, A. J.; Lobo-Castañón, M. J. Aptamer Binding to Celiac Disease-Triggering Hydrophobic Proteins: A Sensitive Gluten Detection Approach. *Anal. Chem.* **2014**, *86* (5), 2733−2739.

(23) Amaya-González, S.; López-López, L.; Miranda-Castro, R.; de-los-Santos-Álvarez, N.; Miranda-Ordieres, A. J.; Lobo-Castañón, M. J. Affinity of Aptamers Binding 33-Mer Gliadin Peptide and Gluten Proteins: Influence of Immobilization and Labeling Tags. *Anal. Chim. Acta* **2015**, *873*, 63−70.

(24) Malvano, F.; Albanese, D.; Pilloton, R.; Di Matteo, M. A New Label-Free Impedimetric Aptasensor for Gluten Detection. *Food Control* **2017**, *79*, 200−206.

(25) Vasilescu, A.; Nunes, G.; Hayat, A.; Latif, U.; Marty, J.-L. Electrochemical Affinity Biosensors Based on Disposable Screen-Printed Electrodes for Detection of Food Allergens. *Sensors* **2016**, *16* (11), 1863.

(26) Miranda-Castro, R.; de-los-Santos-Álvarez, N.; Miranda-Ordieres, A. J.; Lobo-Castañón, M. J. Harnessing Aptamers to Overcome Challenges in Gluten Detection. *Biosensors* **2016**, *6* (2), 16.

DOI: 10.1021/acssensors.7b00810
ACS Sens. XXXX, XXX, XXX−XXX

(27) Labib, M.; Sargent, E. H.; Kelley, S. O. Electrochemical Methods for the Analysis of Clinically Relevant Biomolecules. *Chem. Rev.* **2016**, *116* (16), 9001−9090.
(28) Aghagholizadeh, R.; Kadivar, M.; Nazari, M.; Mousavi, F.; Azizi, M. H.; Zahedi, M.; Rahiminezhad, M. R. Characterization of Wheat Gluten Subunits by Liquid Chromatography − Mass Spectrometry and Their Relationship to Technological Quality of Wheat. *J. Cereal Sci.* **2017**, *76*, 229−235.
(29) Qian, Y.; Preston, K.; Krokhin, O.; Mellish, J.; Ens, W. Characterization of Wheat Gluten Proteins by HPLC and MALDI TOF Mass Spectrometry. *J. Am. Soc. Mass Spectrom.* **2008**, *19* (10), 1542−1550.
(30) Slot, I. D. B.; van der Fels-Klerx, H. J.; Bremer, M. G. E. G.; Hamer, R. J. Immunochemical Detection Methods for Gluten in Food Products: Where Do We Go from Here? *Crit. Rev. Food Sci. Nutr.* **2016**, *56* (15), 2455−2466.
(31) White, S. P.; Dorfman, K. D.; Frisbie, C. D. Label-Free DNA Sensing Platform with Low-Voltage Electrolyte-Gated Transistors. *Anal. Chem.* **2015**, *87* (3), 1861−1866.
(32) White, S. P.; Dorfman, K. D.; Frisbie, C. D. Operating and Sensing Mechanism of Electrolyte-Gated Transistors with Floating Gates: Building a Platform for Amplified Biodetection. *J. Phys. Chem. C* **2016**, *120* (1), 108−117.
(33) White, S. P.; Sreevatsan, S.; Frisbie, C. D.; Dorfman, K. D. Rapid, Selective, Label-Free Aptameric Capture and Detection of Ricin in Potable Liquids Using a Printed Floating Gate Transistor. *ACS Sens.* **2016**, *1* (10), 1213−1216.
(34) Síglez, M. A.; Nocea, B.; del Mar Pérez, M.; Mª García, E.; León, L.; Galera, C. GlutenTox® Pro Test for the Detection of Gluten in Select Foods and Surfaces. *J. AOAC Int.* **2015**, *98* (6), 1608−1627.
(35) Weng, X.; Gaur, G.; Neethirajan, S. Rapid Detection of Food Allergens by Microfluidics ELISA-Based Optical Sensor. *Biosensors* **2016**, *6* (2), 24.
(36) Purohit, S.; Sharma, A.; She, J.-X. Luminex and Other Multiplex High Throughput Technologies for the Identification of, and Host Response to, Environmental Triggers of Type 1 Diabetes. *BioMed Res. Int.* **2015**, *2015*, 326918.
(37) Holding, S.; Wilson, F.; Spradbery, D. Clinical Evaluation of the BioPlex 2200 Celiac IgA and IgG Kits - a Novel Multiplex Screen Incorporating an Integral Check for IgA Deficiency. *J. Immunol. Methods* **2014**, *405*, 29−34.
(38) Lee, K. H.; Kang, M. S.; Zhang, S.; Gu, Y.; Lodge, T. P.; Frisbie, C. D. Cut and Stick" Rubbery Ion Gels as High Capacitance Gate Dielectrics. *Adv. Mater.* **2012**, *24* (32), 4457−4462.
(39) Schalk, K.; Lexhaller, B.; Koehler, P.; Scherf, K. A. Isolation and Characterization of Gluten Protein Types from Wheat, Rye, Barley and Oats for Use as Reference Materials. *PLoS One* **2017**, *12* (2), e0172819.
(40) Kim, S. H.; Hong, K.; Lee, K. H.; Frisbie, C. D. Performance and Stability of Aerosol-Jet-Printed Electrolyte-Gated Transistors Based on Poly(3-hexylthiophene). *ACS Appl. Mater. Interfaces* **2013**, *5* (14), 6580−6585.
(41) Scharnweber, T.; Truckenmüller, R.; Schneider, A. M.; Welle, A.; Reinhardt, M.; Giselbrecht, S. Rapid Prototyping of Microstructures in Polydimethylsiloxane (PDMS) by Direct UV-Lithography. *Lab Chip* **2011**, *11* (7), 1368−1371.
(42) Herne, T. M.; Tarlov, M. J. Characterization of DNA Probes Immobilized on Gold Surfaces. *J. Am. Chem. Soc.* **1997**, *119* (38), 8916−8920.
(43) Jazayeri, M. H.; Amani, H.; Pourfatollah, A. A.; Pazoki-Toroudi, H.; Sedighimoghaddam, B. Various Methods of Gold Nanoparticles (GNPs) Conjugation to Antibodies. *Sens. Bio-Sens. Res.* **2016**, *9*, 17−22.

DOI: 10.1021/acssensors.7b00810
ACS Sens. XXXX, XXX, XXX−XXX